Spring 12-15-2019

SYNTHESIS OF GADOLINIUM-DOXORUBICIN PRODRUG CARRYING FUNCTIONAL NANOCERIA FOR THE TARGETED DRUG DELIVERY AND CANCER TREATMENT

Arth Patel
Pittsburg State University, arthvasantbhai.patel@gus.pittstate.edu

SYNTHESIS OF GADOLINIUM-DOXORUBICIN PRODRUG CARRYING FUNCTIONAL NANOCERIA FOR THE TARGETED DRUG DELIVERY AND CANCER TREATMENT

A thesis submitted to the graduate school
In partial fulfillment of the requirements
for the degree of
Master of Science in chemistry

Arth Patel

Pittsburg State University

Pittsburg, Kansas

July 2020

SYNTHESIS OF GADOLINIUM-DOXORUBICIN PRODRUG CARRYING FUNCTIONAL NANOCERIA FOR THE TARGETED DRUG DELIVERY AND CANCER TREATMENT

Arth Patel

APPROVED:

Thesis Advisor _____
Dr. Santimukul Santra, Department of Chemistry

Committee Member _____
Dr. Jody Neef, Department of Chemistry

Committee Member _____
Dr. James McAfee, Department of Chemistry

Committee Member _____
Dr. Serif Uran, Department of Physics

ACKNOWLEDGMENTS

I want to begin with thanks to my advisor and mentor in my thesis Dr. Santimukul Santra, who gave me this platform to work in his creative lab. His patient, advice, and encouragement made this work possible for me.

I am very grateful to my Parents for supporting me through everything. This would not be possible without them. I also want to thanks my all friends back home which they always believed in me and made me realize how much capable I am.

I am extremely keen to all my lab individuals for being such magnificent buddies through my time at Pittsburg State University. I would also like to thank the Chemistry department for giving me this wonderful opportunity to conduct research.

SYNTHESIS OF GADOLINIUM-DOXORUBICIN PRODRUG CARRYING FUNCTIONAL NANOCERIA FOR THE TARGETED DRUG DELIVERY AND CANCER TREATMENT

An Abstract of the Thesis by
Arth Patel

The main focus of this research was the development of a polymer-coated nanoceria (PNC) platform to be used as a drug delivery system. Water-dispersible PNC is synthesized using a water-based alkaline precipitation method. Cerium nitrate hexahydrate and poly (acrylic acid) are used for the preparation of PNC. The synthesized PNC was characterized using ZETA, and UV- Vis characterization techniques. Polyacrylic acid (PAA)-coated cerium oxide nanoparticles fabricated for the targeted combination therapy of TNBC (MDA-MB-231) and MCF-7. Using EDC/NHS chemistry, the surface carboxylic acid groups of nanoceria was designed and synthesized with ICAM-1 antibody to target ICAM-1 overexpressing TNBC. Next, doxorubicin with gadolinium as a Doxo-Gd prodrug was used as a therapeutic agent. The dialysis technique was used for the purification purpose of nanoparticles to remove unreacted particles. Doxo-Gd provided activable MR imaging and treatment of cancer. The cytotoxicity of the formulated PNC was evaluated using cell-based MTT assays. The cell viability and cell internalization assays were performed using TNBC & MCF-7 cells. The detailed synthetic protocols, characterization data, and experimental results are presented in this work.

TABLE OF CONTENTS

CHAPTER **PAGE**

LIST OF FIGURES

PAGE

LIST OF ABBREVIATIONS

- **PNC:** Polymer-coated nanoceria
- **DOXO:** Doxorubicin
- **TNBC:** Triple Negative Breast Cancer
- **DSP:** Dithiobis(Succinimidyl Propionate)
- **ICAM-1:** Intracellular Adhesion Molecule-1
- **Gd-DTPA:** Gadolinium Diethylenetyramine Pentaacetic Acid
- **PAA:** Poly (Acrylic Acid)
- **EDC:** 1-Ethyl-3-(3-Dimethylaminopropyl) Carbodiimide)
- **NHS:** N-hydroxy Succinimide
- **DMSO:** Dimethyl Sulfoxide
- **PNC-COOH:** Carboxylated Polymeric Nanoparticles
- **PNC-ICAM-1:** Intracellular Adhesion Molecule-1 Coated nanoceria nanoparticle
- **PBS**: Phosphate Buffer Saline
- **DAPI**: 4′,6-Diamidino-2-Phenylindole
- **MRI**: Magnetic Resonance Imaging
- **DLS**: Dynamic Light Scattering
- **MTT**: (3-(4, 5-dimethyl-thiazol-2-yl)-2, 5 diphenyl tetrazolium bromide)
- **ROS**: Reactive oxygen species

Chapter I

Introduction:

Cancer is classified as one of the world's top ten deadliest diseases and it is expected that 606,880 Americans will suffer from cancer growth in 2020.[1] Cancer is a major public health problem worldwide and is the second leading cause of death in the United States. Prostate, lung, and colon cancer represent 42% of all cases in men. Among women, the three most common cancers are breast, lung, and colon cancer. Breast cancer accounts for 30% of all new cancer cases in women.[1] Therefore, cancer needs to be treated with better methods rather than conventional methods and this has been made improvements in the biomedical technology.

The field of biomedical technology is the fastest-growing area in cancer research. [2] The advancement of technology and techniques, has made a vast difference in the pharmaceutical industry.[2] There are many different types of cancer, including: breast, prostate, lung and thyroid cancer. Treating these diseases requires a method of safely delivering therapeutic drugs directly to cancer cells. Before nanotechnology, there were some of the conventional methods like surgery, radiation therapy, and chemotherapy. These methods are still being used in current therapy. However each of these therapies have side effects such a damage to healthy cells, injury to the immune system, and numerous other undesired consequences. It is very important to eliminate the tumor or

cancer cells without spread to other sites of the body.[3] In the last ten years, nanotechnology has provided positive results for treating cancer with lower side effects compared to conventional therapies.[6] When it comes to nanoscience, it is comprised of some unique properties and characteristics, such as low toxicity and early detection of tumor. Nanotechnology and nanoparticles in drug delivery may be the most advanced utilization of nanotechnology in drug delivery in progress. In nanotechnology, particles are designed with the goal that they are attracted to unhealthy cells, which allows direct treatment of those cells.

Role of polymers in drug delivery:

Polymers play an important role in the technology of drug delivery by serving as the framework for the delivery system, encapsulating nontherapeutic molecules like antibodies and dyes, and having a functional surface for targeting cancer cells.[2] In the last two decades the use of polymers in biomedical science has gained solid ground in several applications, such as diagnostic techniques, therapeutic delivery, and controlled drug delivery.[4] Biodegradable polymers find widespread use in drug delivery as they can be degraded to non-toxic monomers inside the body.[3] However, polymers have limitations; for example, natural polymers are plentiful, yet they are difficult to produce synthetically and purify.[2] There are two different types of synthetic polymers; linear polymers and dendritic polymers. A linear polymer is a chain of molecules where all of the bonds of the polymer backbone exist in a single straight line. An example of a linear polymer is Teflon, made from tetrafluoroethylene. It is a single strand of units made from two carbon atoms with two fluorine substituents per carbon atom. The linear polymer cannot store a large amount of drugs because of the lack of pockets in the structure. Branched polymer have

lots of small pockets that can store a variety of drugs and dyes and can deliver safely to the tumor.[3] Dendritic polymers are very stable because of their size and functional surface.[3] These polymer have potential for many applications due to the significant level of control over their physical characteristics, presence of interior cavities, and the likelihood of multivalent interactions as shown in **Figure 1**.[3]

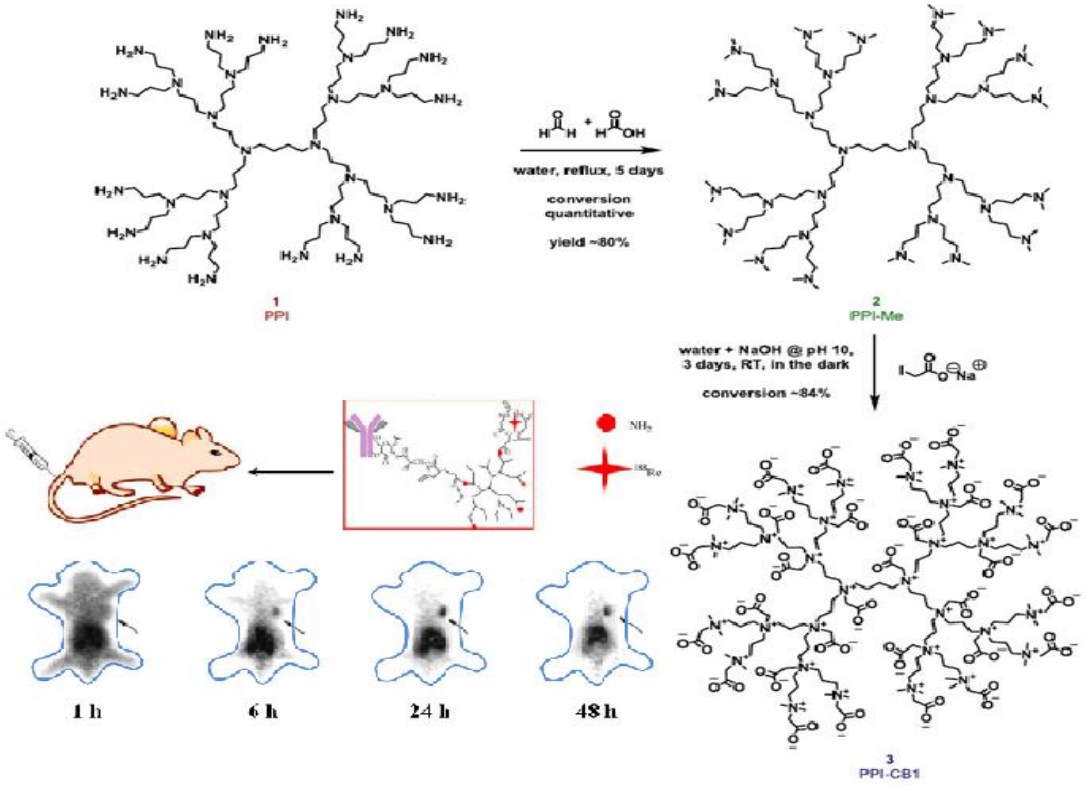

Figure 1: Polypropylene imine generation 3 (G3) dendrimers (in line with the definition by Meijer and co-workers, a PPI dendrimer with 16 end groups is called a third-generation dendrimer.[3]

Role of various nanoparticles in drug delivery:

There are three types of nanoparticles that are used in drug delivery, such as metallic nanoparticles, lipid nanoparticles and polymeric nanoparticles. They all have different methods of synthesis and characteristics. In metallic nanoparticles, there is Iron oxide nanoparticles (IONPs), and Gold Nano nanoparticles (AuNp).

Lipid based nanoparticles:

Many therapeutically effective particles are non-soluble in aqueous systems, chemically and biologically delicate or present severe side effects. Lipid-based nanoparticle (LBNP) systems describe colloidal carriers for bioactive organic molecules.[14, 15] LBNPs such as liposomes, solid lipid nanoparticles (SLN) and nanostructured lipid carriers (NLC) have been considered for drug delivery and cancer treatment. These nanoparticles can transport hydrophobic and hydrophilic molecules, with very low to no toxicity. Liposomes are the most studied delivery systems due to the biocompatibility and biodegradability.[15]The main components of these nanoparticles are phospholipids, which form lipid bilayers as a result of their amphipathic characteristics. The presence of water within the liposomes increases the stability and solubility of anticancer drugs once loaded. In the preparation of liposomes, cholesterol is also an important component. Liposomes are modified with various moieties (e.g., antibodies, peptides, aptamers, and small molecules) that impart specificity and enhance targeting efficiency. For example, RGD (arginine-glycine-aspartic Acid) can be conjugated to a drug delivery vehicle either directly to the surface or via polymeric tethers (e.g., polyethylene glycol). (**Figure 2)**

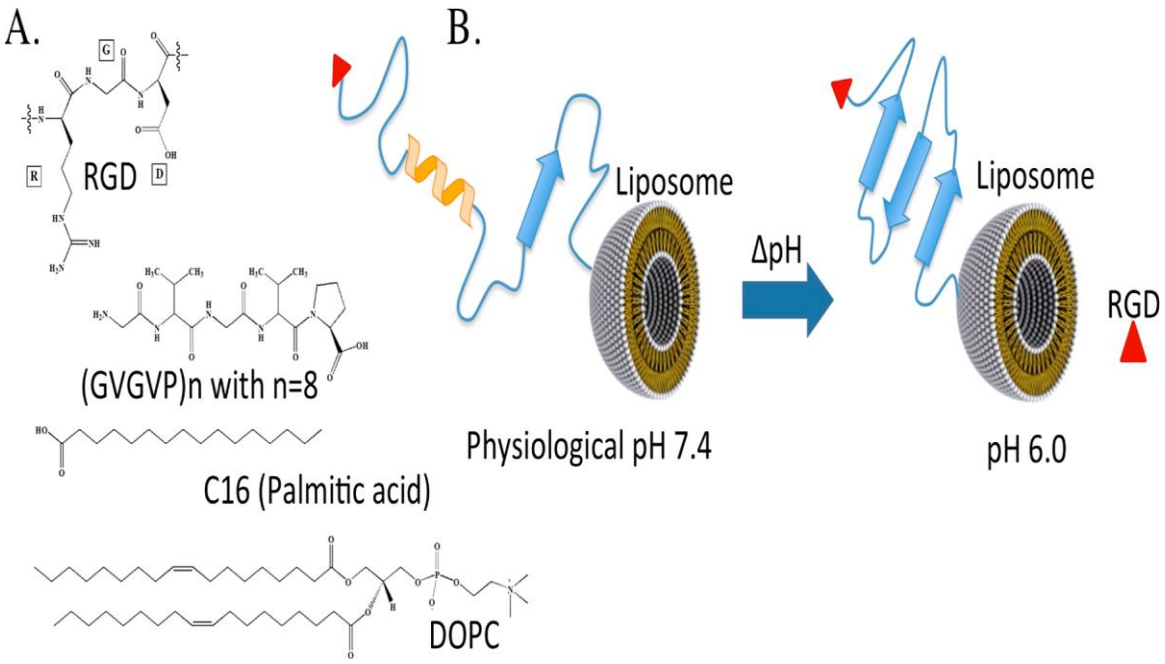

Figure 2: The conformational structure of the elastin-like peptide (ELP) can be used to tune arginine-glycine-aspartic acid (RGD) binding to target breast cancer cells.[15] (A) It is a chemical structures of RGD (targeting head group), ELP (pH-sensitive elastin linker), C16 (hydrophobic anchor tail), and DOPC (lipid).[15] **(B)** It's a mechanism of pH-induced structural conformation of RGD-ELP-modified liposomes.

Iron oxide nanoparticles:

Magnetic nanoparticles (MNPs) are ferromagnetic materials, with small particle size, large specific surface area, and superparamagnetism.[4] In recent years, magnetic nanoparticles (MNPs) have exhibited progress in the field of oncology.[5] The properties of MNPs are exploited when they are utilized as drug delivery vehicles, where drugs may be delivered to specific location in vivo by application of an external magnetic field.[5] Magnetic nanoparticles incorporate properties that make them successful for various biomedical applications, including cell division and recognition, to cell separation and detection, contrast agents in magnetic resonance imaging (MRI), treatment for hyperthermia and drug delivery.[5] Specifically, iron oxide nanoparticles are stable due to their physical and chemical properties like biocompatibility and bio-distribution, strong

magnetic properties, molecular surface groups, and more importantly high stability make it suitable for biomedical applications.[5] Moreover, this detection system can also be extended for detecting biomolecules through new oxidase or peroxidase platforms. The resulting stable iron oxide nanoparticles ionic liquid can be directly used to prepare the millimeter-sized magnetic ionic liquid marble, which when combined with the intrinsic nature of ionic liquids and magnetic properties can be easily transported with an applied magnetic field.[6]

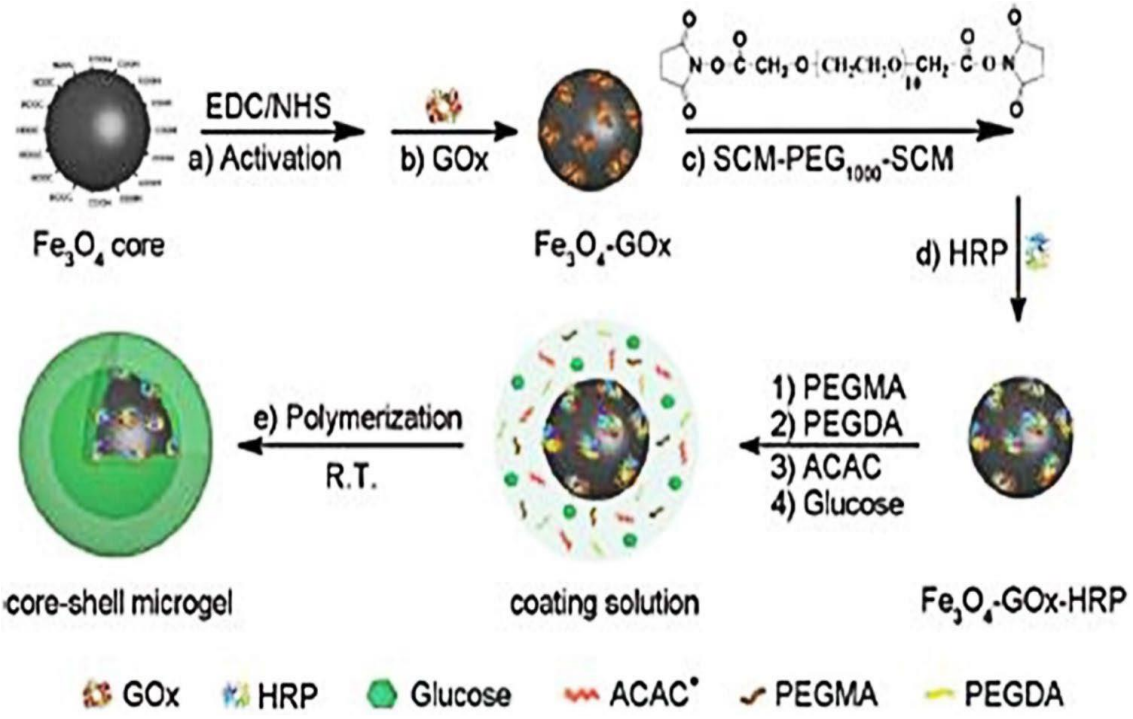

Figure 3: Synthesis of stable iron oxide nanoparticle for biomedical application.[6]

Gold nanoparticles:

Colloidal gold has been valued for its high potential in medicine for long period of time.[7] Gold nanoparticles (AuNp) have advanced properties such as: extensive volume to surface ratio, the possibility for changing surface charge, hydrophilicity, and high surface functionality through surface chemistry. Surface-modified anticancer AuNp causes no to minimal side effects while at the same time providing enhanced drug loading capacity and enhanced blood circulation times. [7,8] An intriguing strategy ensuring the intracellular delivery of active compounds includes their conjugation to the surface of gold nanoparticles through thiol groups. This facilitates the release inside the cell due to the glutathione (GSH) activity and is shown in **Figure 4.**[7] This compound is responsible for removing free radicals and maintaining cellular redox homeostasis due to the capacity to reduce disulfide bonds. Inside the cell, glutathione "removes" molecules conjugated on the surface of AuNP, thus contributing to their efficient release.[7] The chemical properties of AuNPs surface are among the many advantages of AuNPs over other organic and inorganic counterparts. The functionalization of AuNPs surface is easy and highly controllable; thus, the surface chemistry and hydrodynamic diameter of AuNPs, as well as their pharmacokinetics and biodistribution can be appropriately changed through a surface modification.[9,10,12] In addition, the safety profile of AuNPs can be finely tuned by adjusting the size and arrangement of the gold nanocarrier. Studies on AuNPs demonstrated that these nanomaterials do not aggregate in the liver and have no long-term side effects in the animal models.[12,13]

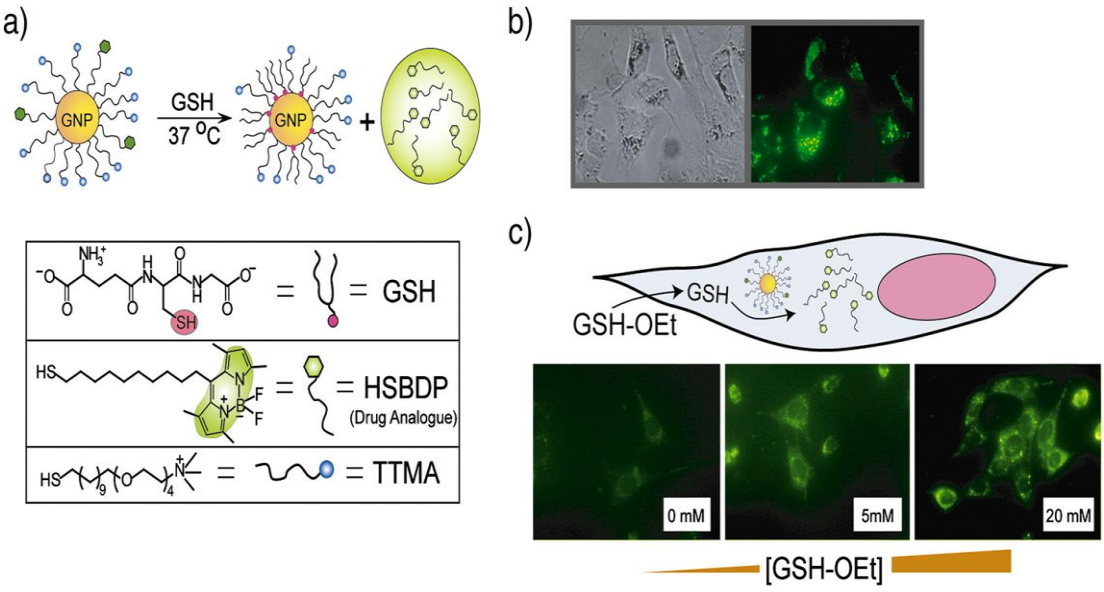

Figure 4: Schematic representation of gold nanoparticles.

Nanoceria (cerium oxide nanoparticle) for drug delivery:

Cerium oxide and polymer-coated nanoceria both has similar properties for drug delivery. Over the last decade, nanoceria has gained much more attention due to its distinctive chemical as well as structural characteristics.[37] Cerium is a rare-earth element from the lanthanide series exists in two oxidation states Ce^{3+} and Ce^{4+}. Nanoceria shows phenomenal antibacterial action against both gram-positive and gram-negative bacteria by means of the increase to reactive oxygen species (ROS).[37] Using nanoceria is a smart option for the elimination of cancer because it can kill cancer cells without damaging healthy tissues. It is theorized that the mechanism of action of nanoceria is that cancerous cells are known to be acidic, and by increase this acidic cell oxidative stress as well as apoptosis, it leads to the destruction of cancer cells.[37] Due to catalytic-activity of nanoceria, it works better in an acidic environment, such as inside a cancer cell. On the other hand, surrounding tissues of cancer remain unharmed because nanoceria works selectively on the cancerous

cells by targeting only the tumor.[39] Due to low pH and high GSH in the endosome, the encapsulated drugs are released into the cytoplasm and then enter either into the nucleus where it binds directly with DNA causing its denaturation, or in mitochondria which increases the production of reactive oxidant species (ROS) that further attack the nucleus and causes the denaturation of DNA, ultimately leading to cell death as shown in **Figure 5.**[38] In this nanoceria as it is very important to control the size, shape and ratio upon which the physical, chemical, and biological attributes depend on it.[37,38] There are numerous methods for the synthesis of nanoceria. These synthetic strategies are fundamental, as the physical and chemical properties depend upon them.[37]

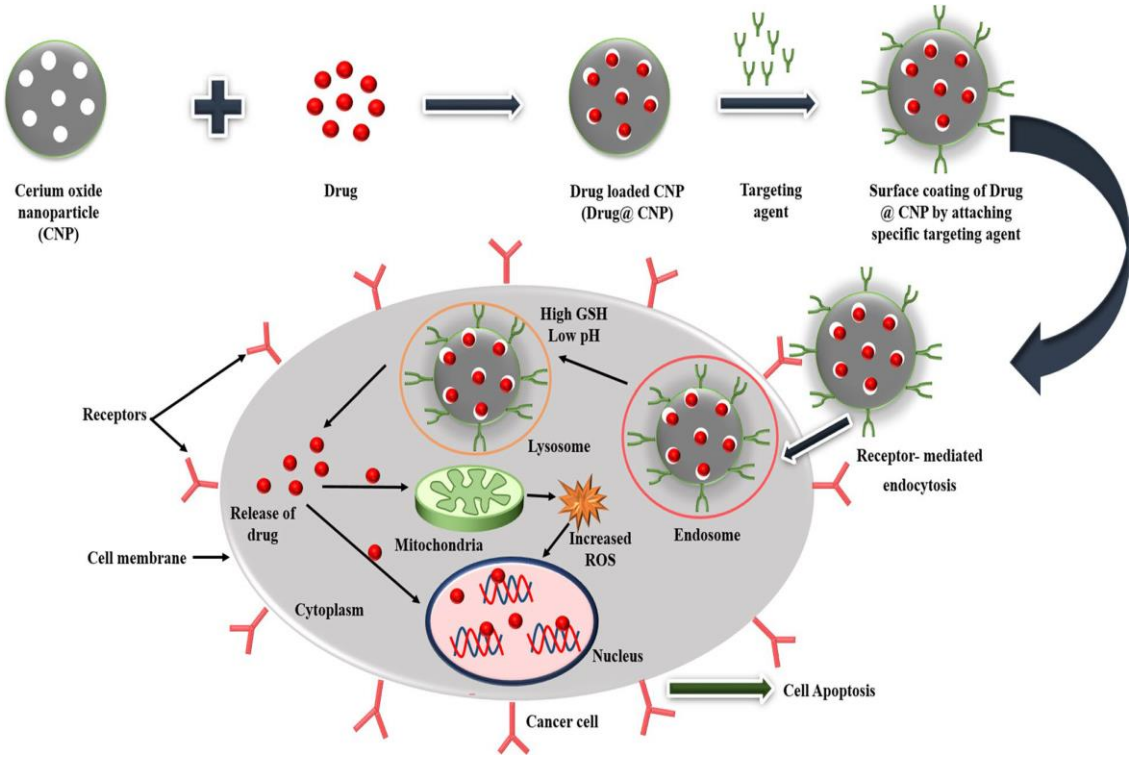

Figure 5: Schematic diagram of drug delivery activity of nanoceria in the cancer cell. Drug CNP coated with specific targeting agents is uptaken by the cell through endocytosis.[38]

Recently, nanoceria has broadly been used in the biomedical field as an effective, targeted drug and gene delivery vehicle. This drug-delivery application of nanoceria in cancer cells has a synergistic anticancer impact because of its absolute cytotoxicity towards cancer cell growth.[37,38] Nanoceria is an innovative way to deal with cancer however there are some drawbacks that need to be addressed which they are stable in a low range of pH which hampers its effectiveness. For this, scientists have been researching to find a feasible approach for its use.

Chapter II

Result and Discussion

Then nanomedicine in this research was designed to provide a platform for focused therapy and MR imaging of triple-negative breast cancer (TNBC). Approximately 10-20% of breast cancers are triple-negative breast cancer.[2] Triple-negative breast cancer is caused by cells that lack specific receptors in their membranes, such as ICAM1.

Focus of this research is to deliver a doxorubicin/gadolinium complex straight to cancer cells with the help of functional nanoceria. This will give MR imaging of ICAM1 overexpressing breast cancer to easily identify those cancer cells while at the same time delivering doxorubicin for combination effect.

Schematic representation of action of nanomedicine inside the cell:

In cancer cells, there is a series of events taking place that can be monitored using magnetic resonance (MR) technique **(Figure 6)**. First, the ICAM1 antibody binds with triple negative breast cancer and is taken in through endocytosis. Once the nanomedicine is inside the TNBC, polymer coated nanoceria becomes distended due to the acidic conditions inside the cell. This releases the prodrug DOXO-SS-Gd from the PNC. Afterward the T1 contrast agent Gd becomes active in the cell due to glutathione (GSH) induced cleavage of the disulfide linker in the prodrug which gives a bright contrast in MR

imaging and the process can be observed. At the same time, doxorubicin becomes activated and has a cytotoxic effect on the TNBC cells. Due to the ability to selectively deliver doxorubicin to TNBC, our nanomedicine has the ability to reduce the side effects of doxorubicin and directly strike tumor cells while monitoring the whole process.

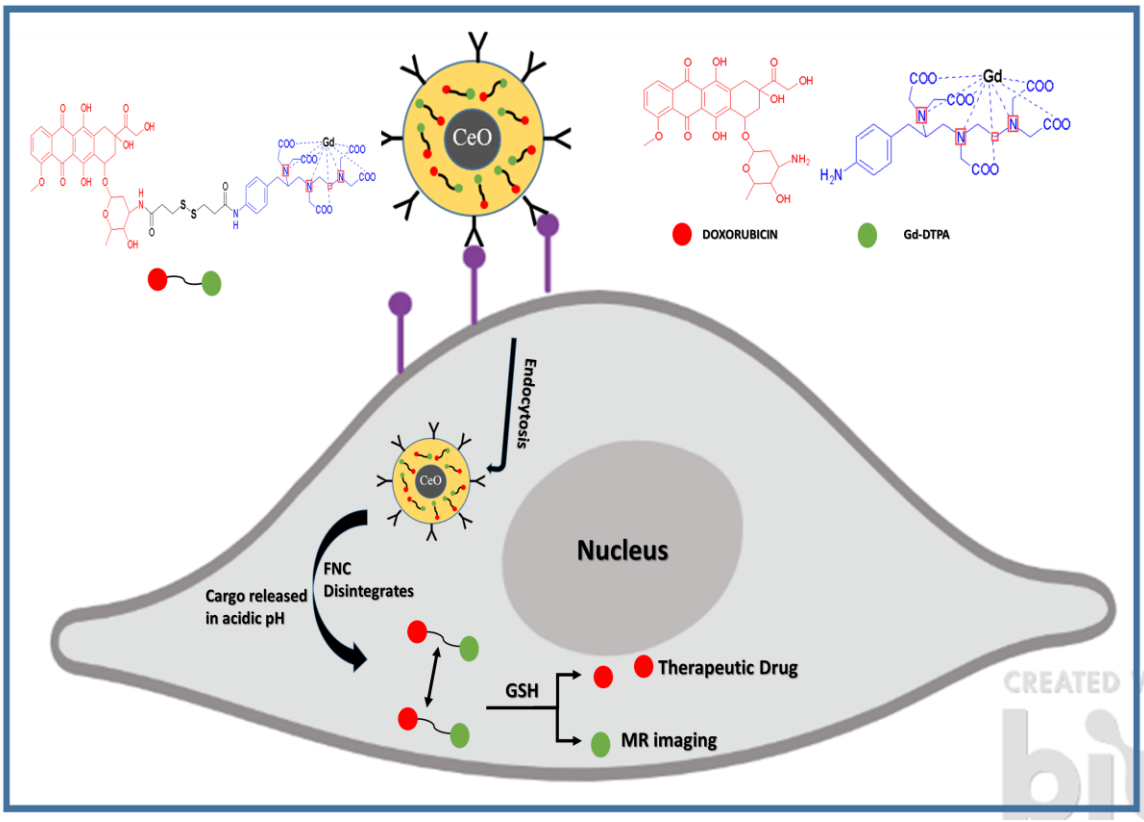

Figure 6: Proposed mechanism of nanomedicine formulated from nanoceria using the Gd-Doxorubicin complex as a prodrug and ICAM1 antibody as a targeting ligand.

Synthesis of DOXO-SS-Gd-DTPA:

The synthesis of DOXO-SS-Gd was carried out by using a procedure that has been reported earlier by using DSP as a crosslinker with the same conjugation method.[44] The prodrug has two major components 1) doxorubicin or Doxo, and 2) gadolinium chelated with diethylenetriamine pentaacetic acid or Gd-DTPA (Gd complex) as shown in **Scheme 1**. Doxorubicin is a type of chemotherapy drug called an anthracycline and it has the ability

to slow or stop the growth of cancer cells by blocking an enzyme called topoisomerase 2. This happens when doxorubicin intercalates with DNA which disrupts the topoisomerase 2 mediated DNA repair mechanism.[45] Gd-DTPA is used as a T1 contrast agent for MR imaging.[46] The, DOXO-Gd prodrug was synthesized and then further encapsulated in functional nanoceria. Once the prodrug is encapsulated into PNC, the T1 MR signals of Gd are quenched due to the presence of strong T2 MR Signals from PNC.

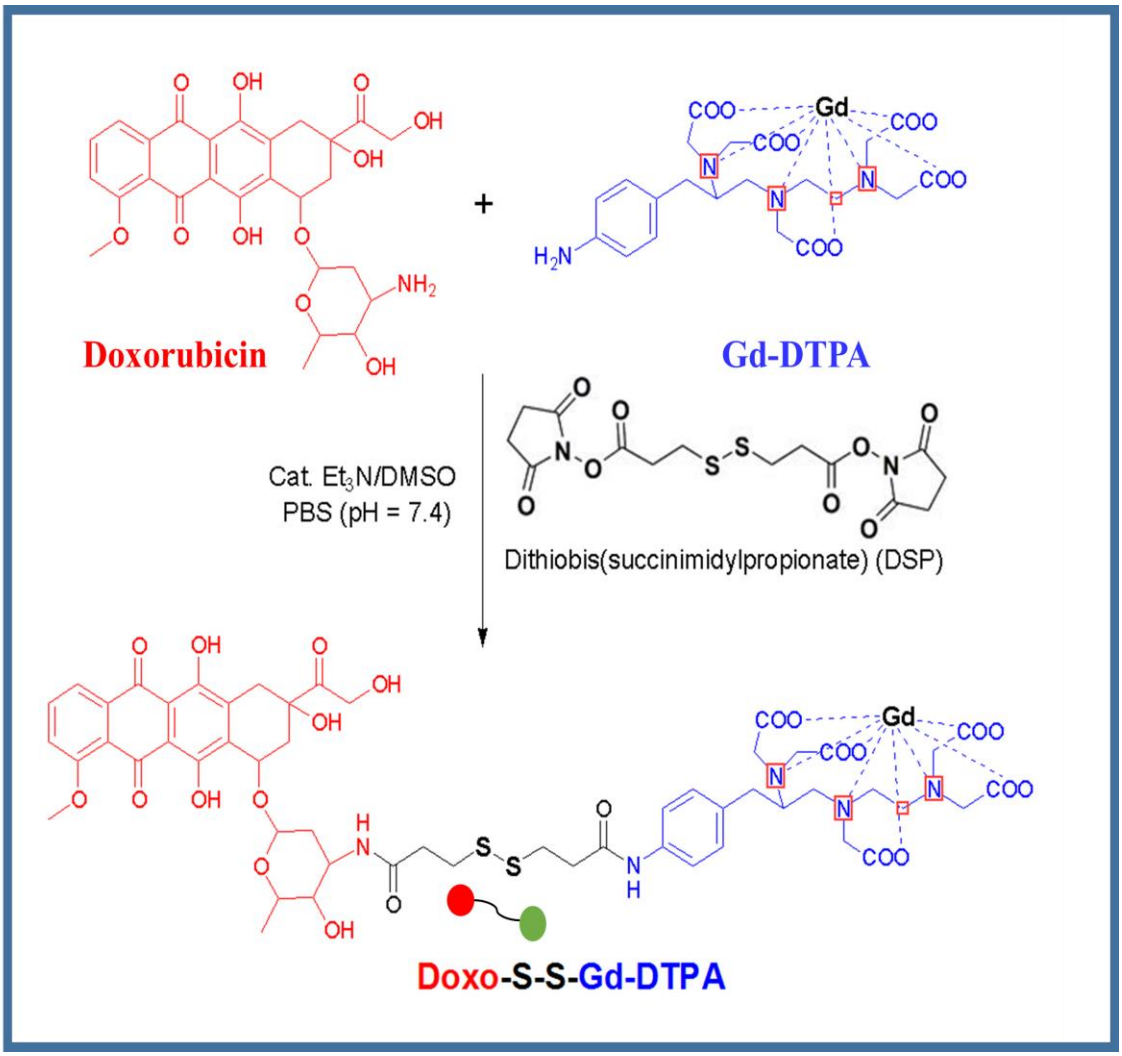

Scheme 1: Synthesis of activable DOXO-SS-Gd-DTPA prodrug.

Characterizations of DOXO-Gd:

The DOXO-SS-Gd prodrug was characterized by examining fluorescence emission and relaxation spectra due to Doxo and Gd, respectively. As per **Figure 7** the maximum absorbance for the prodrug is noted was λ_{abs} = 497nm **(Figure 7A)** and the fluorescence was recorded at λ_{max}= 595 nm. **(Figure 7B).**

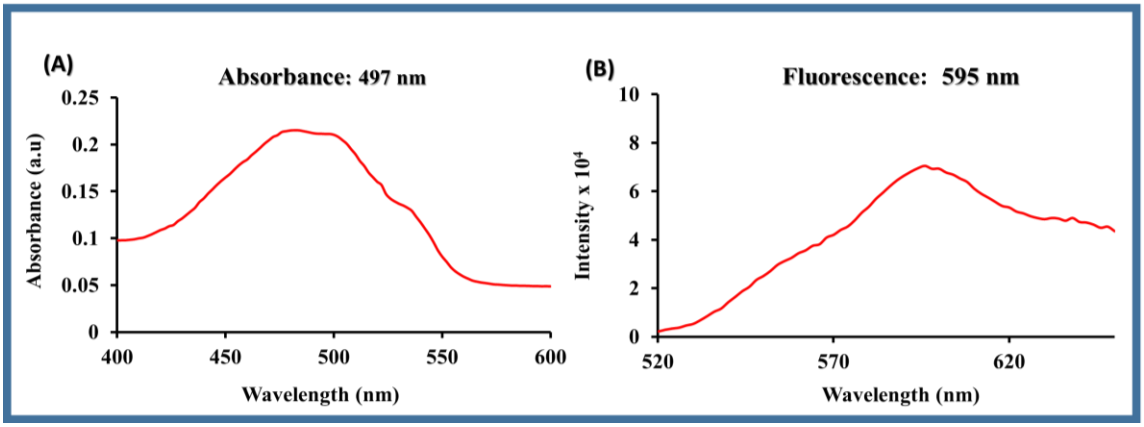

Figure 7: Absorbance and fluorescence of DOXO-Gd (DTPA) activable prodrug.

Synthesis of (PAA)- poly(acrylic acid)-coated cerium oxide nanoparticle:

The polyacrylic acid (PAA)-coated functional nanoceria (PNC) were synthesized using solvent precipitation technique and surface functionalization was carried out by EDC/NHS carbodiimide chemistry **(Scheme 2, 1).** To synthesize nanoceria, a water-based alkali precipitation method was used. Cerium nitrate hexahydrate Ce $(NO_3)_3$ and polyacrylic acid (PAA) were mixed in a 30% ammonium hydroxide solution. PAA works as a stabilizing agent by coating the surface of the formed cerium oxide nanoparticles, stopping the nanoparticles from agglomerating the solution of cerium nitrate hexahydrate and PAA were added to an acidic solution, kept at room temperature, and allowed to react overnight. After 24 h, the reaction mixture was centrifuged 3 times. Next,

the PNC solution was purified using dialysis (MWCO = 6-8 kDa). Dialysis removes the unreacted components that qualifies as an impurity. Functional nanoceria carries two components after encapsulation; 1) doxorubicin an anticancer agent and 2) gadolinium complex (Gd-DTPA).

To conjugate the ICAM1 antibody on surface of PNC-DOXO-COOH (**3**) EDC/NHS chemistry was used. Doxo were encapsulated first in PNC-COOH **(1)** using a vortexer at the speed of 1450 rpm followed by drop wise addition of Doxo-Gd prodrug. After encapsulation of DOXO the solution were kept on mixture at room temperature for 10 h. ICAM1 antibody was dissolve in 1xPBS and quickly added dropwise after addition of EDC & NHS in PNC-DOXO-COOH **(3)** to get surface conjugation of ICAM1 antibody. **(Scheme 2, 4).** After 12 h, prepared solution was dialyzed to remove unreacted and bigger particle in solution. Further absorbance and fluorescence along with zeta & size was recorded for characterization purpose.

DOXO-SS-Gd prodrug was encapsulated into PNC-COOH (**1**) by using a solvent diffusion method. A dilute solution of DOXO-SS-Gd in DMSO was prepared and gradually added to PNC-COOH to obtain PNC-DOXO-SS-Gd **(Scheme 2, 5)**. The hydrophobicity of the prodrug drives it into the nanoparticles which has amphiphilic core. After synthesis, the acquired solution of PNC-DOXO-SS-Gd-COOH **(5)** was purified using magnetic column and dialysis. The final concentration of PNC-DOXO-SS-Gd-COOH found to be 2 mM **(5).**

ICAM1 is known as a specific receptor overexpressed on TNBC cells. Therefore, ICAM1 antibody was functionalized on the surface of PNC by using carbodiimide chemistry to specifically target TNBC cancer cells. As shown in **Scheme 2, 3,** by using

ENC/NHS chemistry PNC was conjugated with ICAM1 antibody on the surface and doxorubicin was encapsulated whiten the core. For using MR purpose Gd was encapsulated with doxorubicin and encapsulated within nanoceria with ICAM1 antibody on the surface **(Scheme 2, 6)**.

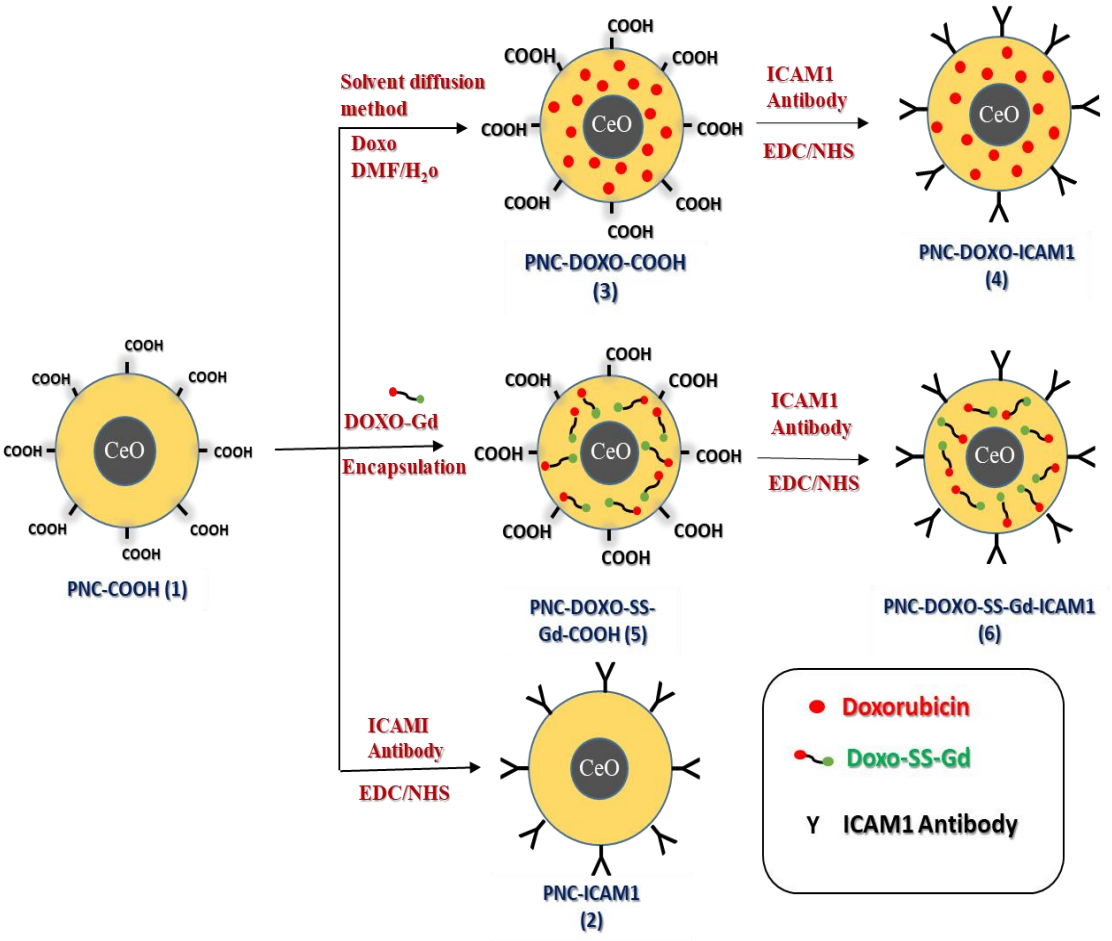

Scheme 2: Synthesis of functionalized Nanoceria-ICAM1 with the help of EDC/NHS chemistry and further synthesis of PNC-DOXO-SS-Gd-ICAM1 using solvent diffusion method.

Characterization study of PNC-COOH-ICAM1:

Furthermore, the purified PNC-COOH-ICAM1 **(1)** was characterized by examining the size and surface charge using dynamic light scattering and zeta-potential determination, As seen in **Figure 8A,** the size of PNC-COOH-ICAM1 was noted to be 46 ± 3 nm and the corresponding zeta potential as per **Figure 8B** was found to be -45 ± 2 mV. Negative zeta potential indicates the presence of carboxylic acid functionality on the surface of the nanoparticles. After characterization, the nanoparticle solution was stored at 4 °C for further use.

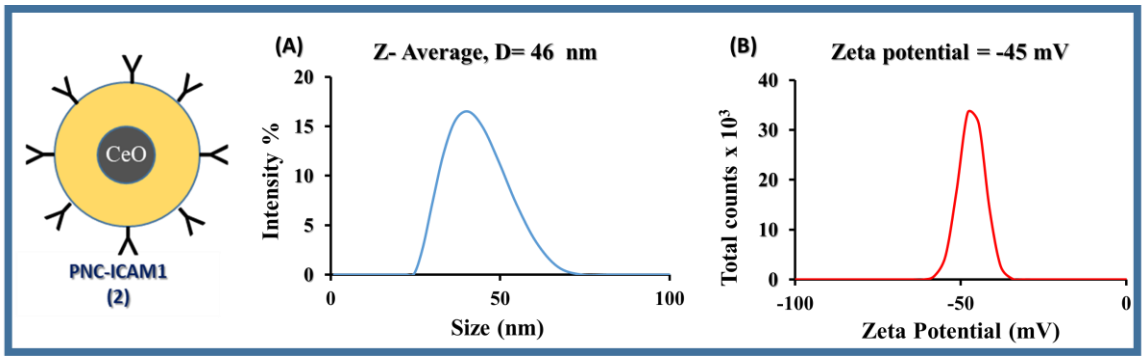

Figure 8: (**A**) The size of PNC-COOH-ICAM1 measured as 49 ± 3 nm and (**B**) zeta potential were measured as -47 mV.

Characterization study of PNC-DOXO-ICAM1:

Afterward, the synthesized PNC-DOXO-ICAM1 was characterized as shown in **Figure 9.** The PNC-DOXO-ICAM1 (**4**) was characterized and, the size and zeta which were noted as slightly increased comparing to PNC-COOH-ICAM1. Size were reported 48 ± 2 nm and zeta of -34 ± 2 mV on the surface indicating a decrease in negative charge on the surface due to successful conjugation of ICAM1 and doxorubicin. Size distribution found to be 48 ± 5 nm. **(Figure 9A)** The surface zeta potential measured was -34 ± 1 mV. **(Figure 9B)**. Absorbance maximum was discovered to be λ_{abs} = 493 nm **(Figure**

9C) and the fluorescence maximum was found to be λ_{max} = 590 nm. **(Figure 9D)** All the characterization results show the successful synthesis of PNC-DOXO-SS-ICAM1 **(4).**

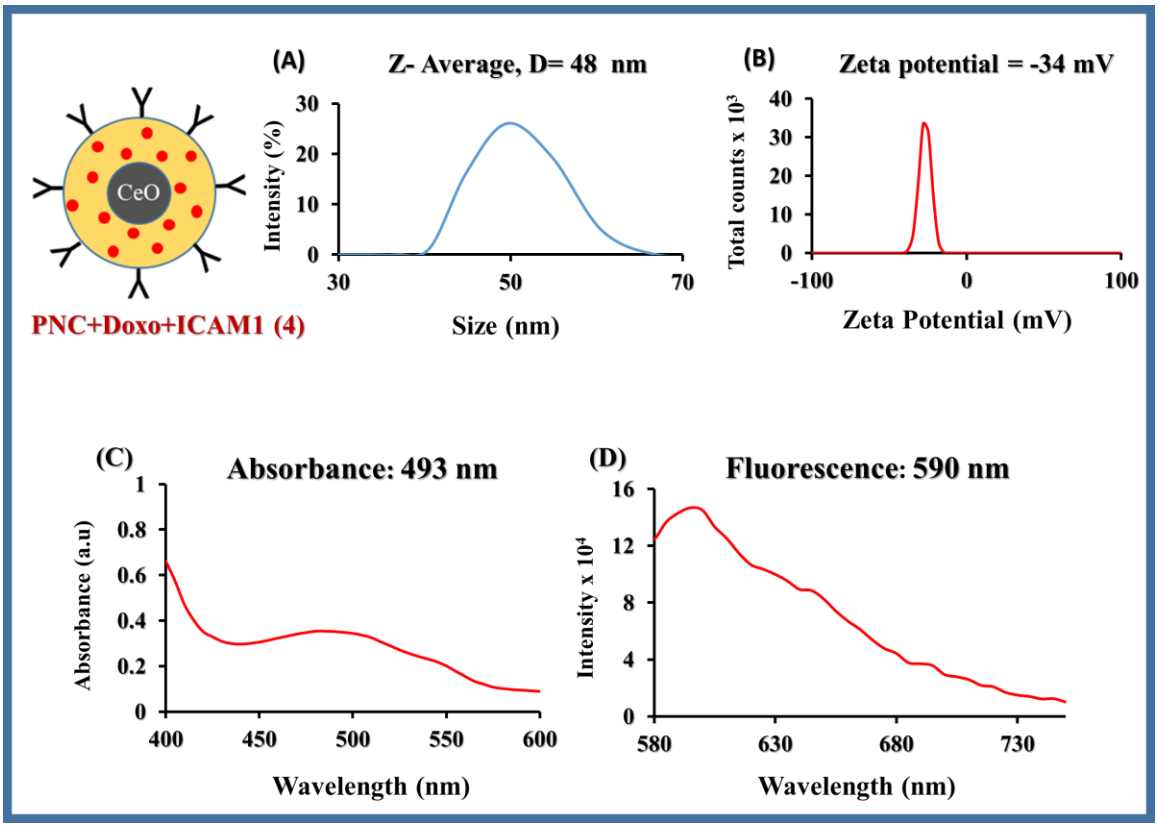

Figure 9: Characterization studies of PNC-DOXO-ICAM1 **(4).**

Characterization study of PNC-DOXO-SS-Gd-ICAM1:

ICAM1 antibody was conjugated to PNC-DOXO-SS-Gd-COOH (**5**) to obtain the nanoparticle of PNC-DOXO-SS-Gd-ICAM1 (**Scheme 2, 6).** This process was conducted by using the method outlined earlier (EDC/NHS chemistry). ICAM1 antibody is used in this targeted delivery because it is overexpressed in cancer cell MDA-MB-231. This nanomedicine includes the features of, chemotherapeutic and MR imaging properties

due to the presence of DOXO-Gd. Hence this nanomedicine can be tested on cells for combination treatment after final solution characterized.

The solution of PNC-DOXO-SS-Gd-ICAM1 **(6)** was characterized to determine the successful conjugation of ICAM1 and the presence of the DOXO-SS-Gd prodrug. First, the size and zeta potential were measured using a method called the dynamic light scattering (DLS). The hydrodynamic diameter of PNC-DOXO-SS-Gd-ICAM1 **(6)** was noted to be 64 ± 2 nm (**Figure 10 A**) and the zeta potential was -18 ± 1 mV (**Figure 10 B**). The increase in size compare to PNC-DOXO-ICAM1 indicated the presence of ICAM1 and DOXO-Gd in PNC **(Figure 10A&10B)**. Additionally, the change in the zeta potential from -47 ± 3 mV (PNC-COOH) (1) to -18 ± 1 mV confirms the surface functionalization of ICAM1. Furthermore, to test the presence of DOXO-SS-Gd, absorbance and fluorescence intensity of PNC-DOXO-SS-Gd-ICAM1 **(6)** were measured. The maximum absorbance was observed at λ_{abs} = 489 nm **(Figure 5C)** and the maximum fluorescence intensity was λ_{max} = 592 nm **(Figure 5D)** indicating the presence of doxo. Furthermore, the relaxation time of the nanomedicine was also tested. The **T1 = 85 ms** was because the signals from Gd were quenched in the presence of PNC. Correspondingly the T2 tested was noted to be **T2 = 279 ms**, indicating the presence of polymeric nanoparticles. Taken together, the characterization data indicates the successful synthesis of the PNC-DOXO-SS-Gd-ICAM1 **(6)** solution.

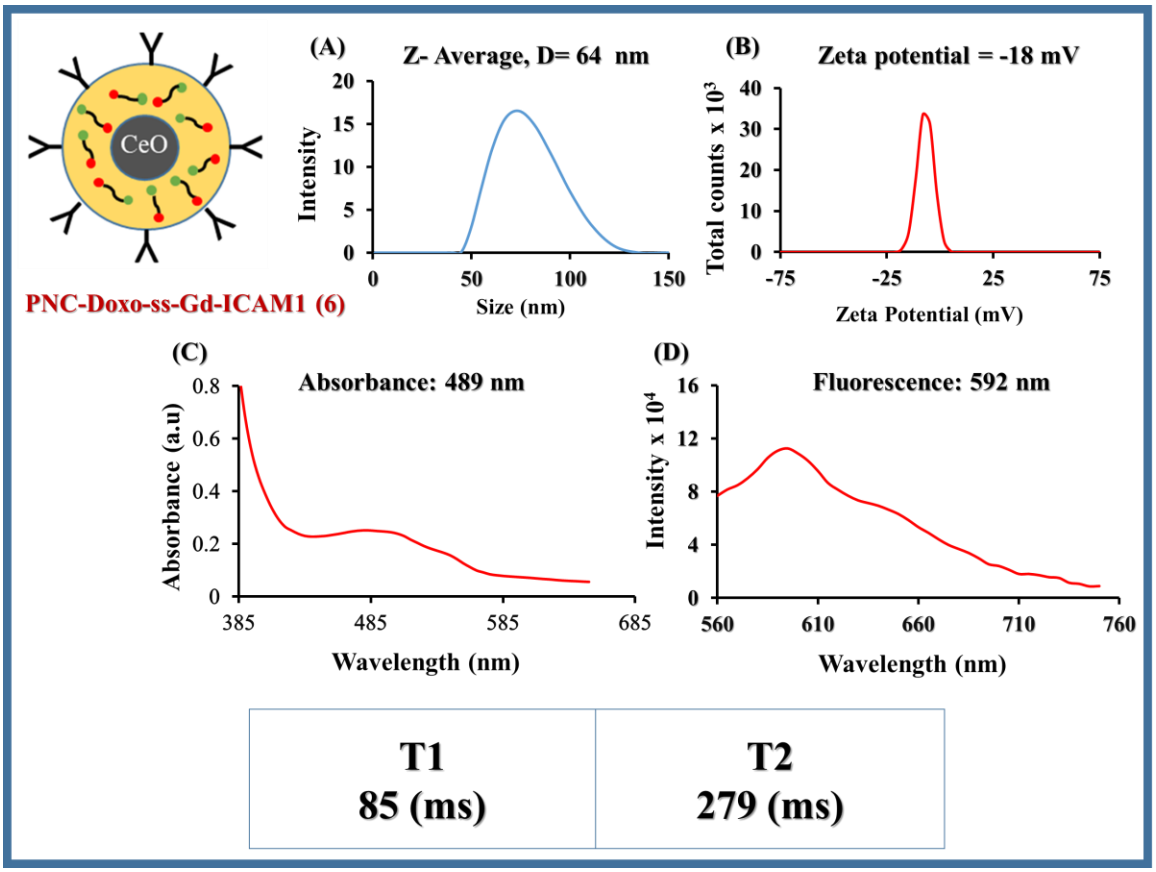

Figure 10: The characteristics of PNC-DOXO-SS-Gd-ICAM1 **(6)** were measured by different types of techniques. DLS studies indicated (**A**) the diameter changed to 64 ± 2 nm and (**B**) the zeta potential was –18 ± 3 mV. Fluorescence studies indicate the (**C**) absorbance to be λ_{abs} = 489 nm and (**D**) fluorescence maxima was λ_{max} = 592 nm. Furthermore, the MR studies suggested the T1 signals T1= 85 ms and the (**F**) T2 relaxation was T2 = 279 ms. Characterization studies ensure the synthesis of PNC-DOXO-SS-Gd-ICAM1 **(6)** was successful.

Cytotoxicity assay using TNBC and MCF-7 cells for 24 h and 48 h:

MTT assay is a standard method to evaluate the cytotoxicity of different therapeutic compounds. The yellow-colored MTT solution transforms into purple color formazan crystals, by mitochondrial reductase, which can only happen in viable cells. In dead cells, the concentration of this enzyme is very low so the reduction of MTT to insoluble formazan does not take place. Thus the absorbance of the formazan is relative to the live cells. In this method, two different nanoformulations were examined for the chemotherapeutic effect.

The solutions tested were 1) PNC-DOXO-SS-ICAM1 **(4)** which is responsible for chemotherapeutic effect while 2) PNC-DOXO-SS-Gd-ICAM1 **(6),** is for the MR imaging with chemotherapeutic effect. Cell viability of TNBC & MCF-7 was measured for 24 h and 48 h post-treatment with these two different nanoformulations. **(Figure 11&12).**

As seen in **Figure 11**, at 24 h and 48 h, by changing the concentration of PNC-DOXO-ICAM1**(4)** and PNC-DOXO-SS-Gd-ICAM1 **(6)** both showed 55% - 60% viability, In contrast, the viability of the control cells (MCF-7) was almost 100% at both 24 h and 48 h with the same concentration for both cell line.

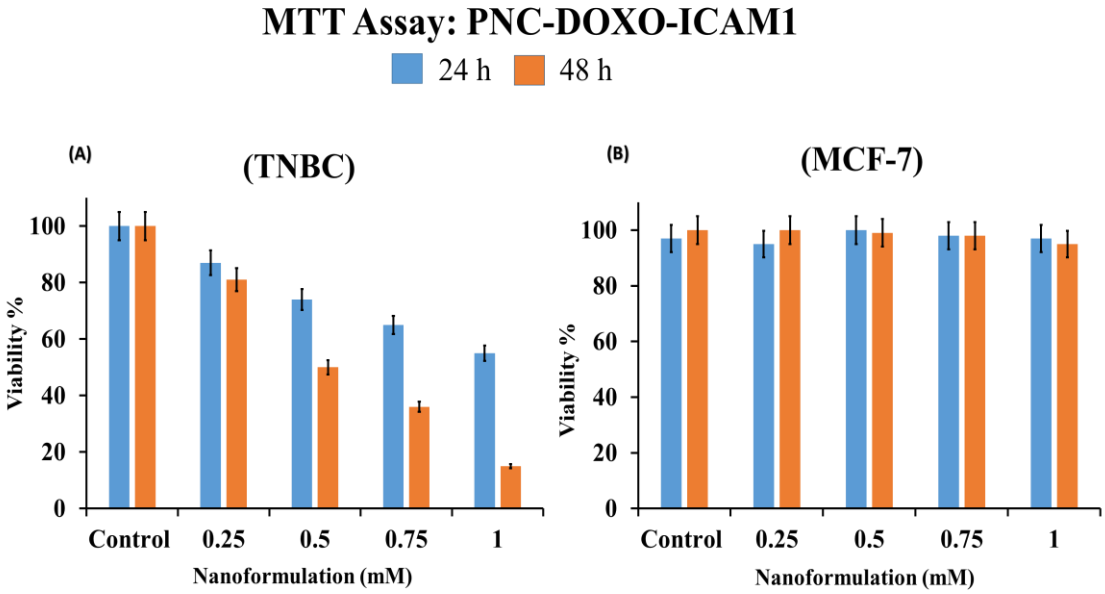

Figure 11: Cell viability assay of TNBC when treated with PNC-DOXO-ICAM1 **(4)** for 24 h and 48 h. Maximum cell death was found to be at 48 h in PNC-DOXO-ICAM1**(4)** treatment. Cell viability assay for MCF-7 shown treatment with different concentrations of PNC-DOXO-ICAM1 **(4)** for 24 h and 48 h. The viability remains nearly constant due to the lack of ICAM1 overexpression in the MCF-7 cell line.

Furthermore, at 48 h the viability of PNC-DOXO-ICAM1 **(6)** and PNC-DOXO-SS-Gd-ICAM1 **(4)** was determined to be very low for TNBC. Doxo is known to damage DNA strands via acting on Topoisomerase 2 at around 36 h. Due to this reason, there is a

drastic decrease in cell viability from 24 h to 48 h upon treatment with PNC-DOXO-ICAM1 **(4)** and PNC-DOXO-SS-Gd-ICAM1 **(6)**. This result shows the potential of PNC-DOXO-SS-Gd-ICAM1, as a chemotherapeutic MR agent.

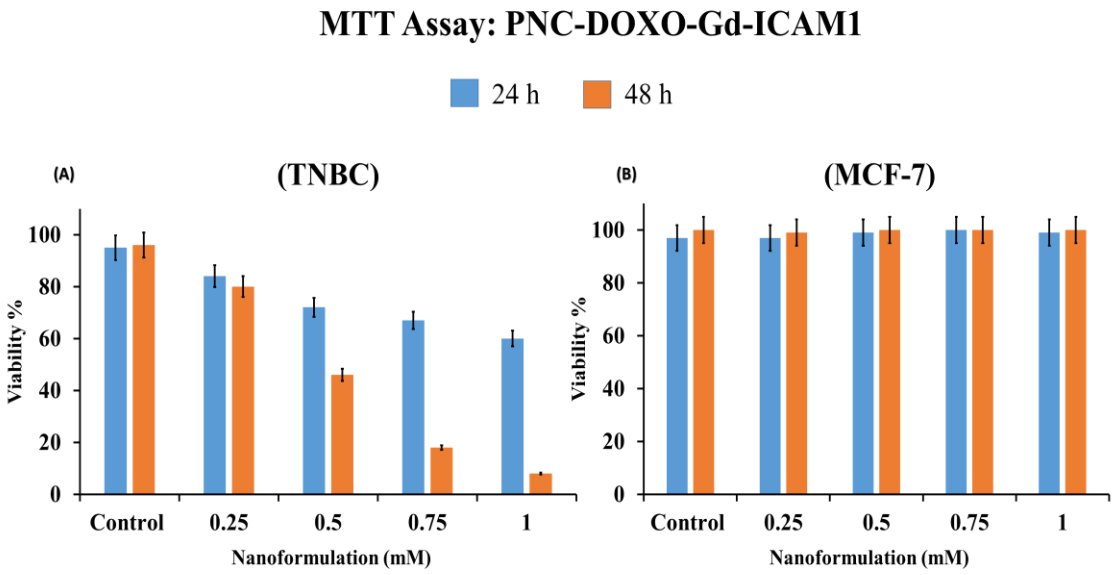

Figure 12: Cell viability assay of TNBC when treated PNC-DOXO-Gd-ICAM1 **(6)** for 24 h and 48 h. Maximum cell death found at 48 h: Cell viability assay for MCF-7 shown treatment with different concentrations of PNC-DOXO-SS-GD-ICAM1 **(6)** for 24 h and 48 h shows negligible cell death due to the lack of overexpressed ICAM1 receptor on MCF-7 cells.

Fluorescence Microscopic Studies: Imaging and Treatment of TNBC and MCF-7 for 24 h and 48h:

To qualitatively visualize the MTT assay of MDA-MB-231, internalization studies were performed. Three different nanoformulations of, PNC-ICAM1 **(2)**, PNC-DOXO-ICAM1 **(4)** and PNC-DOXO-SS-Gd-ICAM1 **(6)** were tested for 24 h and 48 h to observe the changes in cell morphology. Doxorubicin is a known fluorophore and will fluoresce inside the cancer cells. Additionally, the cell nucleus was stained with DAPI to visualize the morphology of the cells. The PNC-ICAM1 **(2)** formulation does not contain doxorubicin for control purpose and so, Dil encapsulated in order to see the cells in this nanoformulation. At 24 h, it was studied upon treatment with PNC-ICAM1 **(2)** fewer cells experienced morphological changes showing the effect of PNC-ICAM1 **(2)** on the viability of cells (**Figure 13 A-D**). Furthermore, when cells were tested with PNC-Doxo-ICAM1 **(4) (Figure 13 E-H**), fewer cells gave the indications of being damaged at 24 h due to the mechanism of doxorubicin action at 36 h, When cells were treated with PNC-DOXO-SS-Gd-ICAM1 **(6),** it shows drastic diminishing in the cell growth **(Figure 13 I-L**), and MCF-7 cells remained confluent and continued growing after the treatment because of the lack of overexpression of ICAM1 **(Figure 13 M-P)**.

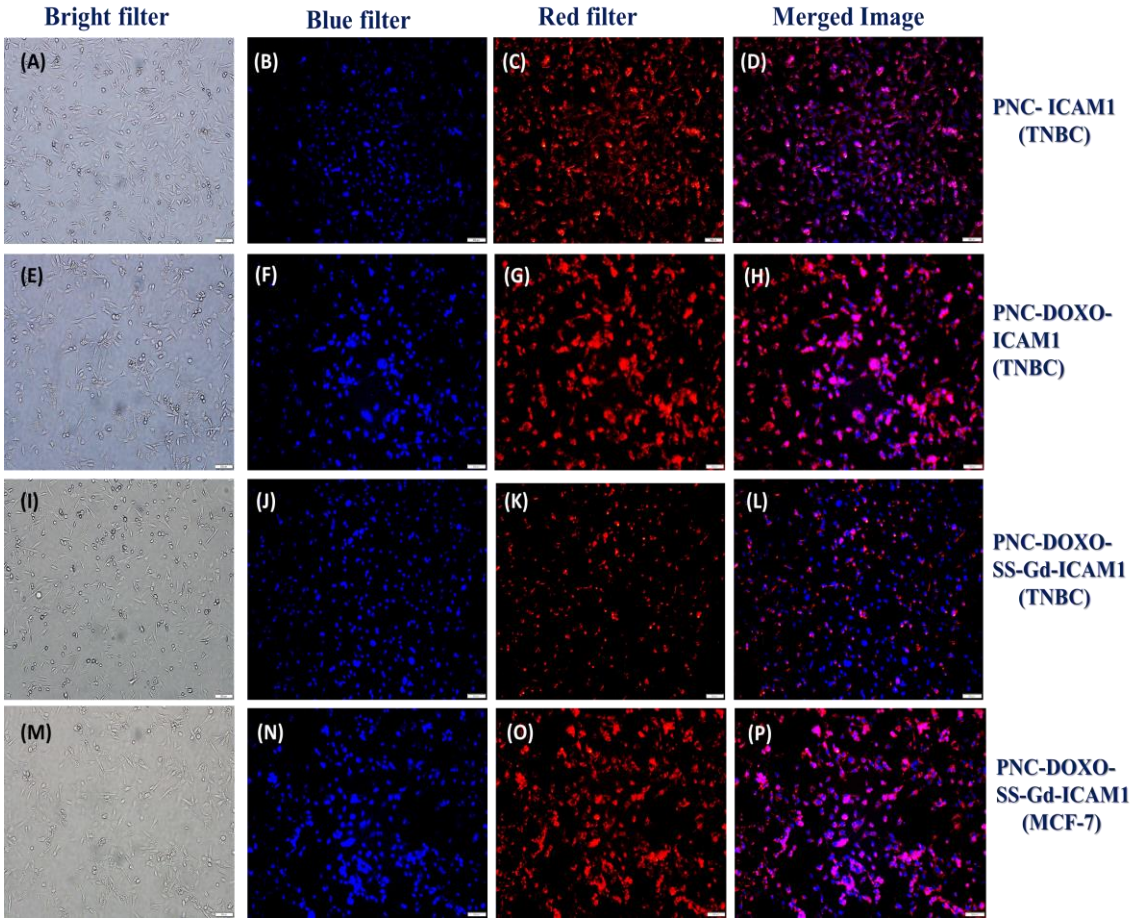

Figure 13. Cell-based fluorescence studies for 24 h: **(13A-13D)** is a portrayal of cells after treatment with PNC-ICAM1**(2**), **(13E-13H)** depicts the treatment of MDA-MD-231 (TNBC) with PNC-DOXO-ICAM1**(4) (13I-13L)** are the microscopic images of MDA-MB-231 (TNBC) upon treatment with PNC-DOXO-SS-Gd-ICAM1**(6)** using blue filter (for DAPI) and a red filter (for Doxo). Figure **(13M-13P)** shows control cells studies of MCF-7.

Fluorescence-based assays were observed at 48 h utilizing the nanoformulations explained above. It was observed that at 48 h, cells show less viability in presence of PNC-ICAM1 **(2) (Figure 14 A-D)**. When cells were treated with PNC-DOXO-ICAM-1 **(4) (Figure 14 E-H)**, due to doxorubicin's action, the cell growth was reduced and most of the cells encountered cell death. For comparison, MDA-MB-231 (TNBC) was subjected to PNC-DOXO-SS-Gd-ICAM1 **(6) (Figure 14 I-L)**, a sharp decrease in the cell growth was

also observed indicating the potent effect of PNC-DOXO-SS-Gd-ICAM1 **(6)**. When MCF-7 were treated with PNC-DOXO-Gd-ICAM1 **(6)** for 48h it remains highly confluent and the lack of overexpressed due to ICAM1. **(Figure 14 M-P).**

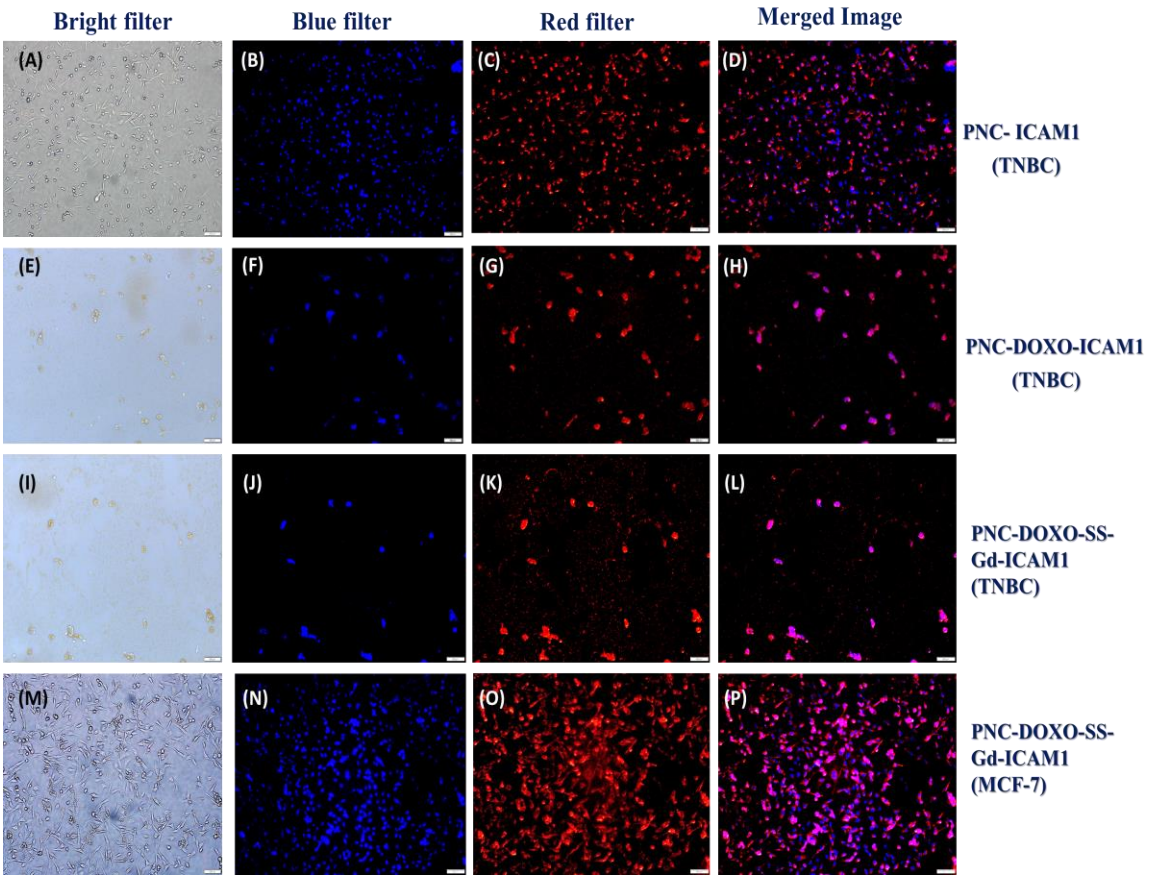

Figure 14: Cellular studies for MDA-MB-231 (TNBC) at 48 h: Images **(14A-14D)** represent the treatment with PNC-ICAM1 (**2**), **(14E-14H)** shows cells treated with PNC-DOXO-ICAM-1 (**4**) and images **(14I-14L)** are the images of cells upon treatment with PNC-DOXO-SS-Gd-ICAM1 (**6**), images **(14M-14P)** shows control cells studies of MCF-7. Each outcome strengthens that our nanosystem is exceptionally proficient in killing cancer cells and has a strong chemotherapeutic effect.

Intracellular Reactive Oxygen Species (ROS) Detection Assay:

In this assay MDA-MB-231(TNBC) cells were producing cytosolic reactive oxygen species (ROS) **(Figure 15)** after being treated with PNC-DOXO-ICAM1 **(4)** nanoparticles. To determine the level of ROS generation, we used dihydroethidium (DHE, 32 μM) dye was used to see ROS in the cytoplasm. Results show once doxorubicin was released into the cytoplasm, generous ROS were produced in the cytoplasm. This is because of doxorubicin binds to cytosolic DNA, generating ROS appearing in **(Figure 15)**. There is insignificant ROS created in cells treated with PNC-ICAM1 **(2)** nanoparticles, demonstrating comparable outcomes to the MTT assay performed. The assays indicated ROS species are generated in TNBC cells when incubated with PNC-DOXO-SS-Gd-ICAM1 **(6)** nanoparticles, ultimately causing cell death.

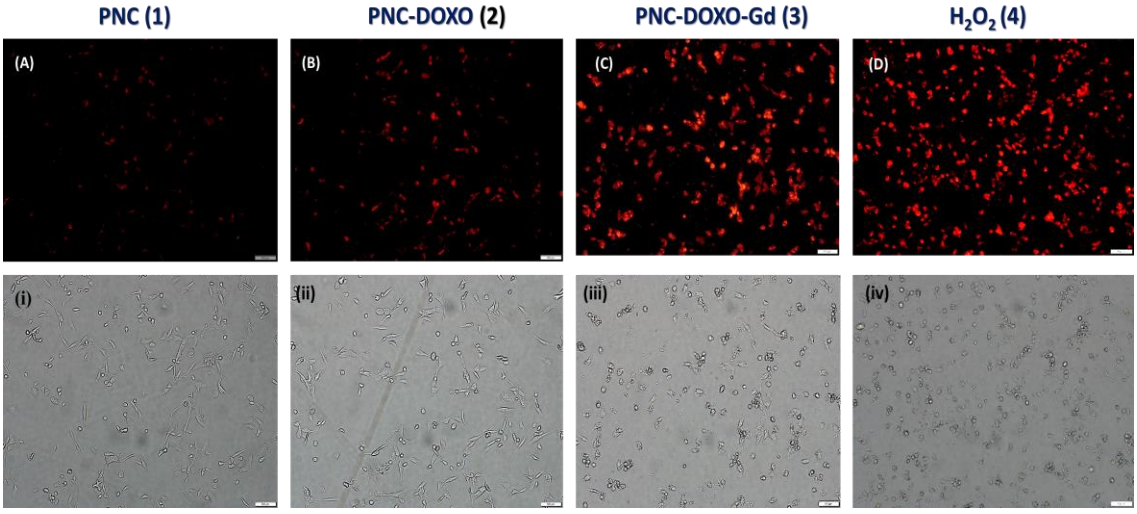

Figure 15: Determination of ROS generation. **(15A−15D)** Fluorescence microscopic images indicating a relative increment in fluorescence from TNBC cells because of the generation of the increased amount of ROS after incubating with PNC, PNC-DOXO-ICAM1 (**4**), PNC-DOXO-Gd-ICAM1 (**6**), and H_2O_2, respectively. Images **(15i−15iv)** are relating to bright-field images.

Comet assay:

Comet assay was carried out to compare the level of DNA damage done to the MDA-MB-231(TNBC) cell line when treated with PNC-DOXO-SS-Gd-ICAM1 **(6)** and PNC-DOXO-ICAM **(4)** (**Figure 16)**. Results indicated both nanoparticles gave no DNA damage in MCF7, as there is no tail indicated as well. However, PNC-DOXO-SS-Gd-ICAM1 **(6)** showed a significant level of DNA damage in TNBC which is comparable to both nanoparticles, Results showed our PNC-DOXO-SS-Gd-ICAM1 **(6)** nanoparticles were effective and gave positive outcomes causing DNA damage to the TNBC cell line.

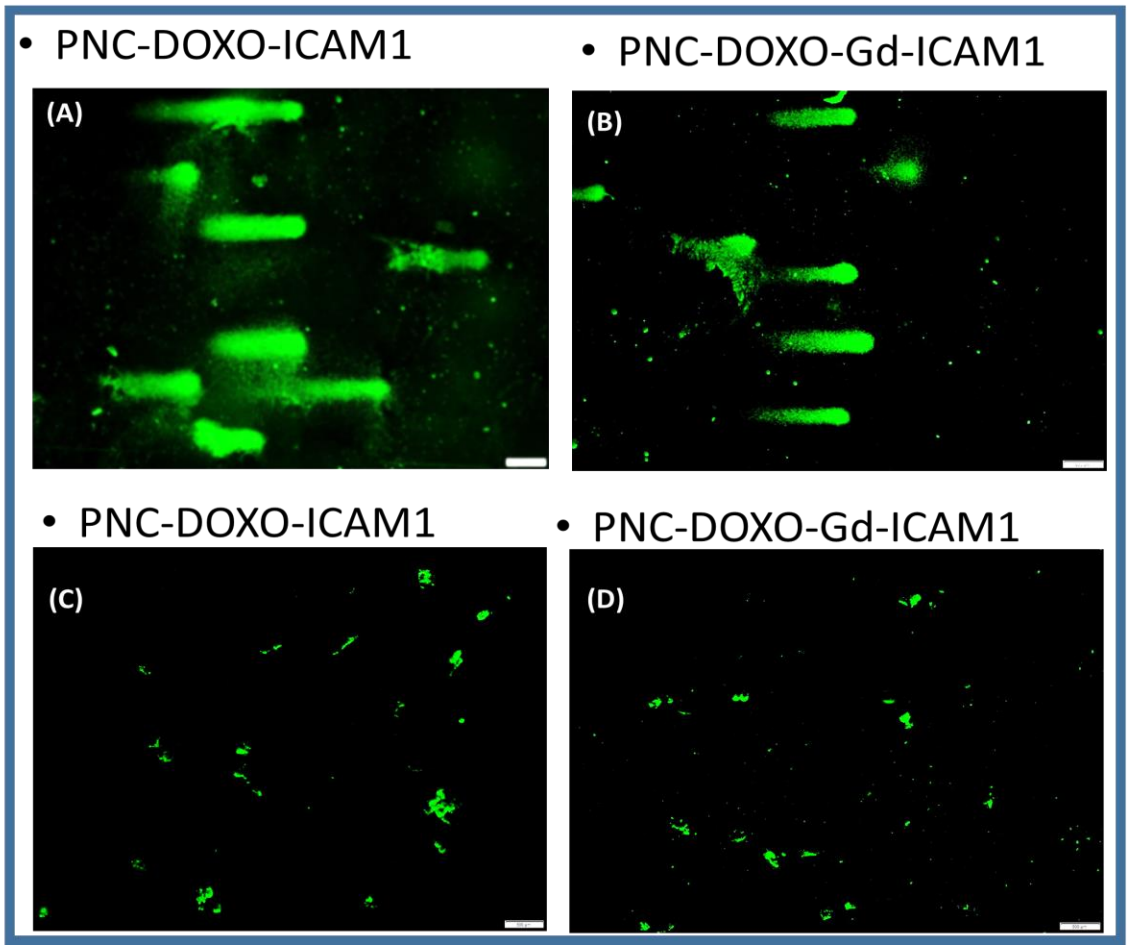

Figure 16: Figure **16A & 16B** shows treatment of two different nanoformulation as shown in figure, it show DNA damage in TNBC and figure **16C & 16D** shows no effects of nanoformulation on MCF 7 which show no DNA damage in it.

Chapter III

Experimental section

1. Materials:

N, N′-dimethyl sulfoxide (DMSO), 2-morpholinoethanesulfonic acid (MES), 1-ethyl-3-(3-(dimethylamino)- propylcarbodiimide hydrochloride (EDC), polyacrylic acid (PAA), chloropropylamine, and 3-(4,5-dimethylthiazol-2-yl)-2,5-diphenyltetrazolium bromide (MTT) were purchased from Sigma-Aldrich and used as soon as received. Near infrared DiI dye and 4,6-diamidino-2-phenylindole (DAPI) dye were purchased from Invitrogen. Cerium nitrate hexahydrate, N-hydroxy succinimide (NHS), ammonium hydroxide, ethanol, isopropanol, and MES sodium salt were purchased from ACROS organics and used without further purification. Doxorubicin was purchased from Alexis Biochemicals and stored at 4 °C for cell based assays. MCF-7 and MDA-MB-231 were bought from ATCC and stored in liquid nitrogen. DSP crosslinker (Dithiobis [succinimidyl propionate]) was obtained from proteoChem and kept at 4^{o} C. ICAM1 (CD54) were purchased from Biolegend and stored at recommended temperature. Dialysis membranes were received from spectrum laboratories. Dihydroethidium (DHE) was obtained from Cayman Chemical, whereas H_2O_2 and para-formaldehyde were received from Electron Microscopy Sciences. Fetal bovine serum (FBS) and 5× annexin V binding buffer were purchased from

BD Biosciences, 70% ethanol, DMEM media and TE buffer were bought from Fisher Scientific.

2. *Synthesis of polymer-coated nanoceria(PNC):*

Cerium nitrate hexahydrate (0.901 g) was dissolved in deionized (DI) water (2.5 mL). This solution were added to 30% ammonium hydroxide solution (30 mL). It was stirred (700 rpm) at room temperature, followed by addition of poly (acrylic acid) (0.905 g) in DI water (10 mL). The color change from brown to dark brown. After 5 min of stirring it turned into deep yellow color after 24 h which indicate stable nanoceria. This reaction was centrifuged three time (20 min each at 3000 rpm) to remove bigger size PNC. The product was purified by dialysis technique using a dialysis bag of molecular weight cutoff (MWCO 6−8K) against DI water.

3. Synthesis of Doxo-SS-Gd prodrug:

DOXO-NH_2 (0.0018 mM) was suspended in DMSO (100 μL) followed by dissolving of Gd-DTPA (1.73 mg) in DMSO (100 μL) (DOXO-NH_2: Gd-DTPA are in 1:1 ratio). Dithiobis (succinimidyl propionate) (DSP) crosslinker (0.744 mg) was dissolved in of DMSO (35 μL). The prepared solutions were mixed and allowed to react for 1 h at room temperature in presence of Et_3N (10 μL). The product obtained was purified to obtain DOXO-SS-Gd prodrug (25 μM). This prodrug was characterized using TECAN fluorescence plate reader Bruker benchtop magnetic relaxometer (MRI).

4. *Encapsulation of Doxorubicin in polymer-coated nanoceria (PNC) using solvent diffusion method:*

DOXO-SS-Gd (25 μM) prodrug was dissolved in DMSO (250 μL). This solution were added in polymer-coated nanoceria solution (4 mL) drop by drop with the vortex speed on 1450 rpm. After this the product were kept on the table mixture for 3 h followed by dialysis in DI water for 2 h to purify the product. The final product were characterized via fluorescence plate reader and DLS and later stored in 4 ^{o}C.

5. Conjugation of ICAM-1 using EDC/NHS chemistry:

EDC (9 mg) (15×10^{-3} mol) was dissolved in MES buffer (150 μL) (100 mM). In addition NHS (6 mg) (15×10^{-3} mol) was dissolved in same MES buffer (150 μL) (100 mM). ICAM1 (5 μL) solution were made in PBS (250 μL) (pH= 7.4). EDC solution were added in two parts in PNC-DOXO-SS-Gd (4 ml) followed by addition of NHS. Prepared solution was mixed gently and 3 min of time were given for reaction to react and after addition of ICAM1 drop wise to create PNC-DOXO-SS-Gd-ICAM1. Further this solution were purified by dialysis technique (MWCO 6−8K) to remove unreacted reagents. PNC-DOXO-SS-ICAM1 (1 mM) was obtained after purification and nanoceria was characterized by Fourier transform infra-red (FT-IR) spectroscopy, overall size and surface charge were measured using dynamic light-scattering (DLS) technique, T1 and T2 relaxation time were measured in magnetic relaxation imaging (MRI).

6. MR imaging studies:

To carry out MR imaging studies a stock solution of PNC-DOXO-SS-Gd-ICAM1 was prepared ([DOXO-SS-Gd] = 25 μM and [PNC] = 2 mM). From this solution five different

dilutions were prepared. The concentrations of Gd were (0.75, 1.5, 2.25, 3.0 and 3.75 μM) prepared for T1 based MR imaging. Similarly, PNC dilutions were prepared with concentrations (5, 10, 15, 20 and 25 mM) for T2 based magnetic resonance imaging.

7. Culture of MDA-MB-231 and MCF 7:

DMEM (Dulbecco's Modified Eagle Medium) media were used by following volume, 85% DMEM-media, 10% fetal bovine serum, and 5% Penicillin/Streptomycin antibiotic to cultivate cells in culture flasks. MDA-MB-231 and MCF 7 cells were trypsinized and seeded in 15 mL tube for centrifuge to get cell pallet. After that cell suspension were made and kept in culture flask in (37 °C, 5 % CO_2) for 24 h. Within 24 to 36 h fully grown cells were split into two different flask. From those flask cells were cultivated as it is for further assays.

8. Cell based fluorescence studies:

The breast cancer cell and MCF-7 cells were seeded into different Petridishes. Once cells become 75% confluent, they were treated with corresponding PNC-ICAM1, PNC-DOXO-ICAM1 (1.0×10^{-3} mol), and PNC-DOXO-SS-Gd-ICAM1 (1.0×10^{-3} mol) for 24 h and 48 h in a humidified incubator (37 °C, 5% CO_2). The cells were washed twice with 1xPBS (pH 7.2) and later fixed with 4% formaldehyde solution for 15 min at room temperature. The cells were then washed once with 1xPBS (pH 7.2) and than cells were treated with 6-diamidino-2-phenylindole (DAPI, 5 mg/mL) dye for staining the nuclei. Cells were washed with 1xPBS (pH 7.2) again and optical images were taken using fluorescence microscope (Olympus IX73).

9. ROS(Reactive oxidant species):

Cells were seeded into different Petridishes at a density of 10,000 cells per well and treated with of various nanoceria preparations (PNC-ICAM1, PNC-DOXO-ICAM1, PNC-DOXO-SS-Gd-ICAM1, H_2O_2) (100 μL) (1.0×10^{-3} mol). After 6 h of incubation at 37 °C, cells were washed twice with 1xPBS (pH 7.2). Then, DHE fluorescent probe (15 μL) was added to each well and incubated for 30 min at room temperature. Cells were washed again twice with 1xPBS (pH 7.2). Subsequently, cells were fixed with 4% paraformaldehyde (1 mL). After fixation, cells were washed with 1xPBS (pH 7.2), stored with of PBS (2 mL) in each well, and the optical images were taken using fluorescence microscope.

10. MTT Assay:

To perform MTT assay MDA-MB-231and MCF7 cells were co-cultured in 96 well plate. For accurate cell numbers of the cells in plate cell pallets were suspended in media (4 mL) and from that only 1 mL solution were used and added additional DMEM media (9 mL) for exactly 2500 cells in each well. After culturing cells subsequently nanoformulation (PNC-ICAM1, PNC-DOXO-ICAM1, PNC-DOXO-SS-ICAM1) (30 μL) (1.0×10^{-3} mol) were added and kept in incubator for 24 and 48 h with different set of concentration. After treatment period media suspension from the wells were removed and wash each wells with 1xPBS. Subsequently, MTT (30 μL) (5 mM)solution was added and plates were placed in the incubator (37 °C, 5 % CO_2) for 4-6 h. Purple colored formazan crystals were produced and solubilized with isopropyl alcohol. Result were measured at wavelength between 520 to 570 nm using the TECAN microplate reader. Similar procedure was carried out and MTT method were followed for control cells MCF-7.

11. Comet assay:

For performing comet assay, TNBC cells were harvested on 12 well plate (8,000 cells/well). Cells were treated with all nanoformulation (PNC-ICAM1, PNC-DOXO-ICAM1, PNC-DOXO-SS-ICAM1) (1.0×10^{-3} mol), (5, 60 µL, [Fe] = 2.5×10^{-3} mol) and incubated for 24 h. After that cells were centrifuged at 1200 rpm for 6 min to collect damage cells. Cell pellet was resuspended in 1xPBS (pH 7.2) and blended in with pre-warmed low-dissolve agarose at 1:10 proportion. This agarose blend (100 µL) was placed on the comet slide. The slide was then at first kept in the dark at 4 °C for 1 h, in the lysis solution. Alkaline electrophoresis (Trevigen) was made on the following day according to manufacturer suggested protocol. Quickly, slides were kept in alkaline unwinding solution (pH>13) and electrophoresis was completed for 30 min at 21 V. The slides were then washed twice with DI H_2O and 70% ethanol, separately. Next, slides were stained with SYBR Gold for 15 min in dark and afterward dried at 37 °C for 20 minutes. Images were taken utilizing the FITC filter on the Olympus IX73 fluorescence magnifying instrument.

Chapter IV

Conclusion and Future Directions:

Functional nanoceria were successfully synthesized as a drug-delivery vehicle with a Doxo-Gd for the treatment of TNBC. ICAM1 decorated nanoceria were formulated for the targeted delivery of combination of drugs, Doxo and Gd. Different cell-based tests showed the capability of nanoformulation for killing the triple negative breast cancer (TNBC) cells while having no effect on normal cells. The nanoformulations demonstrated excellent drug load capacity as shown by the encapsulation studies, stability, reduced toxicity, and higher therapeutic efficacy. Furthermore, as shown in ROS, MTT and Cell based fluorescence assays shows an excellent effect of Doxo-Gd encapsulated nanoformulation which proves that it is successfully going inside the TNBC cell due to ICAM1 overexpression and killing TNBC cell while having no effect on MCF7 which has no expression of ICAM1. The tests utilizing MR imaging demonstrated the nanoformulation can be used to analyze cancer growth and further screen the MR based cancer treatment.

Furthermore comet assay showed the effects of two different nanoformulation which proves that Doxo-Gd encapsulated nanoceria has more DNA damage in TNBC cell indicating more distort tail in the result. Nanoparticles can successfully be used as a model for the focused double treatment (chemotherapy and MR imaging) and analysis of TNBC

cells. In addition, this model can be customized for focusing on different cancer cell lines. After a firm foundation of in vitro settings, this model can be tried in-vivo to more readily comprehend its working inside a living system. In addition, this model can possibly be analyzed for different kind of tumors for the dual-targeted treatment and diagnosis purposes.

REFERENCES.

1. Rebecca L. Siegel MPH Kimberly D. Miller MPH Ahmedin Jemal, *A cancer journal for clinicians*, **2019**,111-120.

2. William B. Liechty, David R. Kryscio, Brandon V. Slaughter, Nicholas A. Peppas, Polymers for Drug Delivery Systems, *Bimolecular Eng vol, 1*, Aug **2010**,149-173.

3. Esther Roeven, Luc Scheres, Maarten M. J. Smulders, Han Zuilhof, Design, Synthesis, and Characterization of Fully Zwitterionic,Functionalized Dendrimers, *ACS omega, 11*, **2019**,243-250.

4. Hangzhou, Zhejiang, P.R, Meijia Wu, Shengwh Huang, China Magnetic nanoparticles in cancer diagnosis, drug delivery and treatment, *Molecular and clinical oncology*, *12*, **2017**, 738-746.

5. Laís Saloao Arias, Juliano Pelim Pessan, Ana Paula Miranda Vieira, Taynara Maria Toito de Lima, Alberto Carlos Botazzo, Delbem ID and Douglas Roberto Monteiro, Iron oxide nanoparticles for biomedical application, *Antibiotics*, 17, **2018,** 311-315.

6. Niemirowicz, Markiewicz, K.H Wilczewska, A.Z Car, H. Magnetic nanoparticles as new diagnostic tools in medicine. *Adv. Med, 06,* **2012**, 57, 196–207.

7. Krzysztof Sztandera, Michał Gorzkiewicz, and Barbara Klajnert-Maculewicz,Gold nanoparticles in cancer treatment, *Mol. Pharmaceutics*, **2019**, *1*, 1-23.

8. Muhammad U. Farooq, Valentyn Novosad, Elena A. Rozhkova, Hussain Wali, Asghar Ali, Ahmed A. Fateh, Purnima B. Neogi, Arup Neogi & Zhiming Wang, Gold Nanoparticles-enabled Efficient Dual Delivery of Anticancer Therapeutics to HeLa Cells. *Sci Rep, 13,* **2018**, 2045-2322.

9. Li SD, Huang L, Pharmacokinetics and biodistribution of nanoparticles. *Mol Pharmaceutics*, **2008,** 496-504.

10. Movia D, Gerard V, Maguire CM, A safe-by-design approach to the development of gold nanoboxes as carriers for internalization into cancer cells, *Biomaterials, 35,9* ***2014***, 2543-57.

11. Spadavecchia J, Movia D, Moore C, Manus Maguire C, Moustaoui H, Casale S, Volkov Y, Prina-Mello A, Targeted polyethylene glycol gold nanoparticles for the treatment of pancreatic cancer from synthesis to proof-of-concept in vitro studies. *Int J Nanomedicine, 11,* **2016**, 791-822.

12. Razzak R, Zhou J, Yang X, The biodistribution and pharmacokinetic evaluation of choline-bound gold nanoparticles in a human prostate tumor xenograft model, *Clin Invest Med*, 21, **2013,** 133–E142.

13. You J, Zhou J, Zhou M. Pharmacokinetics, clearance, and biosafety of polyethylene glycol-coated hollow gold nanospheres, *Part Fibre Toxicol*, 19, **2014**,11-26.

14. García-Pinel, Beatriz, Lipid-Based Nanoparticles: Application and Recent Advances in Cancer Treatment, *Nanomaterials*, *vol 9,* Apr **2019,** 638.

15. Eleftheria Veneti, Raymond S. Tu, and Debra T. Auguste, *Bioconjugate Chemistry*, *27, **2016**,* 1813-1821.

16. Malvindi MA, De Matteis V, Galeone A, Brunetti V, Anyfantis GC, Athanassiou A, Toxicity assessment by silica coated iron oxide nanoparticles, *PLoS One*, *13*, **2014**.

17. Wongwailikhit, K, Horwongsakul, S. Mater. Lett, The preparation of iron (III) oxide nanoparticles using W/O microemulsion, *Materials Lett*, *Vol 65,* **2011**, 2820–2822.

18. Maity, D. Ding, J. Xue, J.M. Funct, Mater. Lett. Synthesis of magnetite nanoparticles by thermal decomposition Time, temperature, surfactant and solvent effects, *Functional Materials Letters 1, 3,* **2008**, 189-193.

19. Reddy, L.H. Arias, J.L. Nicolas, J. Couvreur, P. Magnetic nanoparticles Design and characterization,toxicity and biocompatibility, pharmaceutical and biomedical applications, *Chem. Rev*, 112, **2012**, 5818–5878.

20. Sun, Y. Chen, Z.L. Yang, X.X. Huang, P. Zhou, X.P. Du, Magnetic chitosan nanoparticles as a drug delivery system for targeting photodynamic therapy. *Nanotechnology*, *20*, **2009**, 135102.

21. Alupei, L. Peptu, C.A. Lungan, A.M. Desbrieres, J. Chiscan, O. Radji, S. Popa, New hybrid magnetic nanoparticles based on chitosan-maltose derivative for antitumor drug delivery, *Int. J. Biol. Macromol*, 92, **2016**, 561–572.

22. Lee, J. H. Choi, S. U. S. Jang, S. P. Lee, S. Y. Production of Aqueous Spherical Gold Nanoparticles Using Conventional Ultrasonic Bath, *Nanoscale Res. Lett*, *7*,**2012**, 420.

23. Fleming, D. A. Williams, M. E. Size-Controlled Synthesis of Gold Nanoparticles via High-Temperature Reduction, *Langmuir*, 20, **2004**, 3021−3023.

24. Sujitha, M. Kannan, S. Green, Synthesis of Gold Nanoparticles Using Citrus Fruits, Citrus Limon, Citrus Reticulata and Citrus Sinensis Aqueous Extract and Its Characterization, *Spectrochim. Acta*, 102, **2013**, 15−23.

25. Shao, Y. Jin, Y. Dong, Synthesis of Gold Nanoplates by Aspartate Reduction of Gold Chloride, *Chem. Commun, 9,* **2004**, 1104−1105.

26. Connor, E. E. Mwamuka, J. Gole, A. Murphy, C. J. Wyatt, M.D, Gold Nanoparticles Are Taken up by Human Cells but Do Not Cause Acute Cytotoxicity, *Small*, 1, **2005**, 325−327.

27. De Jong, W. H. Hagens, W. I. Krystek, P. Burger, M. C. Sips, A. J. A. M. Geertsma, R. E, Particle Size-Dependent Organ Distribution of Gold Nanoparticles after Intravenous Administration, *Biomaterials*, *29*, **2008**, 1912−1919.

28. Huang, X. Jain, P. K. El-Sayed, I. H. El-Sayed, M. A. Gold Nanoparticles Interesting Optical Properties and Recent Applications in Cancer Diagnostics and Therapy, *Nanomedicine, 2,5,* **2007**,681−693.

29. Chen, Y. S. Hung, Y. C. Liau, I. Huang, G. S, Assessment of the in Vivo Toxicity of Gold Nanoparticles, *Nanoscale Res. Lett*, 4, 8, **2009**, 858−864.

30. Obeid, M.A. Tate, R.J. Mullen, A.B. Ferro, V.A, Lipid-Based Nanoparticles for Cancer Treatment, Elsevier Inc. Amsterdam, The Netherlands Lipid nanocarrier, *William Andrew Publishing*, 52, **2018**, Pages 139-174.

31. Wang, W. Zhang, L. Chen, T. Guo, W. Bao, X. Wang, D. Ren, B. Wang, H. Li, Y.Wang, Anticancer effects of resveratrol-loaded solid lipid nanoparticles on human breast cancer cells, *Molecules,* 22, **2017**, 1814.

32. Angelova, A. Garamus, V.M. Angelov, B. Tian, Z. Li, Y. Zou, A. Advances in structural design of lipid-based nanoparticle carriers for delivery of macromolecular drugs, phytochemicals and anti-tumor agents, Adv. *Colloid Interface Sci*, 249, **2017**, 331–345.

33. M. Oliver, M. R. Jorgensen, and A. D. Miller, The facile solid-phase synthesis of cholesterol-based polyamine lipids, *Tetrahedron Letters, vol. 45*, **2004**, 3105–3107.

34. Y. Zhao, L. Huang, Lipid nanoparticles for gene delivery, *Adv. Genet*, *88*, **2014,** 13–36.

35. Kuchma, M. H, Phosphate ester hydrolysis of biologically relevant molecules by cerium oxide nanoparticles, *Nanomedicine, 6,* **2010**, 738–744.

36. Kaittanis, S. Santra, Asati, Perez, J. M. A, cerium oxide nanoparticle-based device for the detection of chronic inflammation via optical and magnetic resonance imaging. *Nanoscale*, 23, **2012**, 2117–2123.

37. Wason MS, Zhao J, Cerium oxide nanoparticles Potential applications For cancer and other diseases, *Am J Transl Res, 26,* **2001**,126-131.

38. Thakur, N. Manna, J. Das, Synthesis and biomedical applications of nanoceria, a redox active nanoparticle, *J Nanobiotechnology,17,84*, **2019**.

39. Xu C, Qu X, Cerium oxide nanoparticle a remarkably versatile rare earth nanomaterial for biological applications, *NPG Asia Mater, 11,* **2014**.

40. Vinardell M, Mitjans M, Antitumor activities of metal oxide nanoparticles, *Nanomaterials, 5*, **2015**, 1004-1021.

41. Syed Abdul Kuddus, Nanoceria and Its Perspective in Cancer Treatment, Department of Pharmaceutical Science, North South University Bangladesh, Dhaka, *J. Pharm. Sci, 31,* **2001**,1229.

42. A.S. Karakoti, N.A. Monteiro-Riviere, R. Aggarwal, J.P. Davis, R.J. Narayan, W.T. Self, J. McGinnis, and S. Seal, Nanoceria as Antioxidant: Synthesis and Biomedical Applications, *JOM*,**2014,** 13-20

43. Teles RHG, Moralles HF, Cominetti MR, Global trends in nanomedicine research on triple negative breast cancer a bibliometric analysis, *Int J Nanomedicine, 13,* **2018**, 2321-2336.

44. Gao L, Yu J, Liu Y, Tumor-penetrating Peptide Conjugated and Doxorubicin Loaded T1-T2 Dual Mode MRI Contrast Agents Nanoparticles for Tumor, *Theranostics, 8,* **2018,** 92-108.

45. S. Santra, S. Jativa, C. Kaittanis, G. Normand, J. Grimm, J. Perez, , Gadolinium-Encapsulating Iron Oxide Nanoprobe As Activatable NMR/MRI Contrast Agent, *ACS Nano*, 6, **2012**, 7281-7294.